Hindawi
International Journal of Chemical Engineering
Volume 2022, Article ID 4613023, 12 pages
https://doi.org/10.1155/2022/4613023

Research Article

Sensitivity Analysis with the Monte Carlo Method and Prediction of Atenolol Removal Using Modified Multiwalled Carbon Nanotubes Based on the Response Surface Method: Isotherm and Kinetics Studies

Mohammad Mehdi Amin,[1,2] **Nasrin Bagheri**,[1,3] **Farzaneh Mohammadi**,[1] **and Bahare Dehdashti**[1,2,3]

[1]*Department of Environmental Health Engineering, School of Health, Isfahan University of Medical Sciences, Isfahan, Iran*
[2]*Environment Research Center, Research Institute for Primordial Prevention of Non-Communicable Disease, Isfahan University of Medical Sciences, Isfahan, Iran*
[3]*Student Research Committee, School of Health, Isfahan University of Medical Sciences, Isfahan, Iran*

Correspondence should be addressed to Bahare Dehdashti; baharehdehdashty@yahoo.com

Received 28 February 2022; Accepted 17 May 2022; Published 8 June 2022

Academic Editor: Vikranth Kumar Surasani

Atenolol (ATN) is a β-blocker drug extensively used to treat arrhythmias and high blood pressure. Because the human body cannot metabolize it completely, this drug has been commonly found in many environmental matrices. In the present study, the response surface method (RSM) was used for adsorption prediction of ATN on modified multiwalled carbon nanotubes (M-MWCNTs) by NaOCl and ultrasonic. The sensitivity analysis was done by the Monte Carlo method. Sensitivity analysis was performed to determine the effective parameter by the Monte Carlo simulator. Statistical analysis of variance (ANOVA) was performed by using the nonlinear second-order model of RSM. The influential parameters including contact time (min), adsorbent dosage (g/L), pH, and the initial concentration (mg/L) of ATN were investigated, and optimal conditions were determined. Kinetic of ATN adsorption on M-MWCNTs was evaluated using pseudo-first, pseudo-second-order, and intraparticle diffusion models. Equilibrium isotherms for this system were analyzed by the ISOFIT software. As per our result, optimum conditions in the adsorption experiments were pH 7, 60 min of contact time, 0.5 mg/L ATN initial concentration, and 150 mg/L adsorbent dose. In terms of ATN removal efficiency, coefficients of R^2 and adjusted R^2 were 0.999 and 0.998, respectively. Sensitivity analysis also showed that contact time has the greatest effect on increasing the removal of ATN. Pseudo-first-order (R^2 value of 0.99) was the best kinetic model for the adsorption of ATN, and for isotherm, BET (AIC_C value of 3.27) was the best model that fit the experimental data. According to the obtained results from sensitive analysis, time was the most important parameter, and after that, the adsorbent dose and pH affect positively on ATN removal efficiency. It can be concluded that the modified multiwalled carbon nanotubes can be applied as one of the best adsorbents to remove ATN from the aqueous solution.

1. Introduction

β-Blockers are an important group of drugs extensively used to treat arrhythmias and high blood pressure. ATN, bisoprolol, metoprolol, sotalol, and propranolol are common kinds of β-blockers [1], among which ATN is widely used for the therapy of cardiovascular disease, hypertensive disease, infantile hemangioma [2], acute myocardial infarction [3], and decline the intensity of heart attacks. Approximately 50% of the amount ingested by humans cannot be metabolized during excretion, and it is frequently detected in urban wastewater [4]. Researchers expressed conventional wastewater treatment plants (WWTPs) including ozonation and microbial transformation [5] cannot remove ATN

sufficiently. Thus, this leads to the increasing occurrence of ATN in different water bodies [2] such as surface waters, ground waters, and hospital wastewaters in the last decade [6]. Researches showed ATN concentration in the effluent was about 0.78–6.6 mg/L, whereas the admittable level is 10 ng/L [7]. Studies demonstrate that this compound is resistant to biodegradation and therefore can remain in the matrix for long time [6] and has a toxic effect on aquatic microorganisms and humans [1]. Moreover, after a chlorination process, ATN illustrated phytotoxic activity [2]. Consequently, ATN removal from aqueous solution is important. Recently, scientists use some methods for ATN removal including oxidation with UV/peroxydisulfate [8], oxidation with light [6], chlorination/UV process [9, 10], and ozonation [2]. Generation of toxic by-products [5] and high energy consumption [4] are drawbacks of the last methods.

Nowadays, adsorption is widely used because of easy operation, low cost, high efficiency, and lack of toxic by-products for removal of contaminants from the aqueous solution [11]. So far, among applications of various adsorbents, carbon nanotubes (CNTs) also have been extensively used due to the large specific surface area, high porosity, and high reaction activity [11–13]. The most well-known carbon nanotubes are single-walled (SWCNTs) and multiwalled (MWCNTs) [12]. To improve performance and increase the efficiency of CNTs, two methods such as acid treatment and ultrasonication are applied [14]. MWCNTs modified by nitric acid have been used as adsorbents for removal of diclofenac from aqueous solution in China [15]. Ncibi et al. investigated the removal of antibiotic pharmaceutical from aqueous solutions by using single and multiwalled carbon nanotubes optimized by ultrasonic. They found the application of ultrasound help CNTs for omitting of drugs [16].

The objective of this study was to investigate the removal of atenolol by multiwalled carbon nanotubes modified with NaOCl and ultrasonic. The equilibrium isotherms and kinetics of the ATN-M-MWCNTs adsorption system have been determined and analyzed using several adsorption models. Also, in order to determine relationships between parameters and the effects on removal of the pollutant, the RSM model was used. In the following, by using sensitivity analysis with the Monte Carlo method, impacts of the evaluated parameters on the response parameter were determined.

2. Materials and Methods

2.1. Materials. All chemicals including ATN ($C_{14}H_{22}N_2O_3$) with a purity of ≥98%, NaOCl (70%), HCl (≥37%), and NaOH (≥98%) were prepared from Merck Co., Germany. Raw MWCNTs (Cheap Tubes Inc., USA) was used as the base adsorbent. Table 1 provides the physical and chemical characteristics of the selected carbon nanotubes.

2.2. Adsorption Experiments. The preparation of adsorbent was explained in our last study [7]. The stock solution of 1,000 mg/L of atenolol was made by 100 mg of pure atenolol and deionized water. The tests were carried out under 25°C and in 100 mL dishes including 50 mL of the sample. The initial concentration of ATN for each stage of the experiment was 0.5, 1, 5, and 10 mg/L. The pH value (2, 4, 7, and 11) was managed by adding HCl or NaOH solutions and was measured by a pH meter (CyberScan pH1500, Thermo Fisher Scientific Inc., The Netherlands). The adsorbent dosages of 50, 100, 150, and 200 mg/L were added to the solutions at each stage. In order to proper mixing of the adsorbate and adsorbent, the solutions were placed on a shaker (orbital shaker, model OS 625, Germany) for 5, 20, 60, and 90 min, at the rate of 250 rpm. In all of the study steps, ATN solutions without any adsorbents were used as controls. So, ATN adsorption on the bottle wall or through evaporation was insignificant. After a certain contact time, the samples were filtered with a filter (CA0.22), and the nanoparticles were separated. After that, the samples were centrifuged at 10,000 rpm (Universal 320, Hettitech, Germany) for 10 min. Finally, ATN concentration was analyzed by the high-performance liquid chromatography (HPLC).

Table 1: Specifications of MWCNTs used in this study.

Characteristics	Values
Purity	>95%
Outer diameter	<8 nm
Inner diameter	2–5 nm
Length	>10 μm
Specific surface area	>500 $m^2 \cdot g^{-1}$
Electric conductivity	>100 $s \cdot cm^{-1}$
Tap density	0.27 $g \cdot cm^{-3}$
True density	2.1 $g \cdot cm^{-3}$

2.3. Measurements and Data Analyzing. The samples were prefiltered by the 0.45 μm PTFE hydrophilic sterile filter, Membrane Solutions, MS® CA Syringe Filter Company, USA. ATN concentrations in the aqueous solution before and after the treatment were measured by the Waters HPLC, with a UV-486 detector at a wavelength of 231 nm (Waters Company, USA). The HPLC mobile phase was a combination of 0.01 M potassium dihydrogen orthophosphate with a pH value of 3.5 and acetonitrile with a volumetric ratio of 60 : 40. An isocratic method with a flow rate of 1 mL/minute and a sample injection volume of 20 μL, stationary phase (column) (250 × 4.6 mm; 5 μm) C18-Waters-Spherisorb®, and oven temperature of 25°C was used; the results of the calibration curve of atenolol within the concentration range of 0.1–10 mg/L in the water matrix revealed the linearity of the measurement method, with a correlation coefficient (R^2) as large as 0.99.

Shape, size, and surface morphology of MWCNTs and M-MWCNTs were investigated through transmission electron microscopy (TEM). Moreover, to determine the functional groups and formation of chemical bonds in MWCNTs and M-MWCNTs, the FTIR spectrometer was used (Bruker Optics, TENSOR 27, Netherlands).

The ATN removal efficiency (E, %) and adsorption capacities (q, mg/g) of M-MWCNTs were calculated according to the following equations [17]:

$$E = \frac{C_o - C_e}{C_o} \times 100, \quad (1)$$

$$q = \frac{(C_O - C_e)V}{m}, \quad (2)$$

where C_o and C_e (mg/L) are the initial and equilibrium ATN concentrations, respectively, $V(L)$ is the volume of the solution, and m(g) is the mass of each used adsorbent.

2.4. RSM Modeling and Sensitivity Analysis. The RSM model is widely used in laboratory studies modeling [18]. This method is a complete collection of statistics methods to evaluate the parameters effect and interaction of them on response variable and to search for optimum condition [19]. In this study, the relationship between independent variables and response variables by quadratic models in the RSM model is expressed as [20]

$$y = \beta_0 + \sum_{i=1}^{k} \beta_i X + \sum_{i=1}^{k} \beta_{ii} X_i^2 + \sum_{i=1}^{k} \sum_{i \neq j=1}^{k} \beta_{ij} X_i X + \varepsilon. \quad (3)$$

According to equation (3), y is the excepted response, $X_{i.j}$ coded the independent variables, k is the number of variables, β_0 is the model constant, β_i represent the coefficients of linear variables, β_{ii} represent the coefficients of variables with quadratic, β_{ij} represent the coefficients of variables interaction, and ε is the error rate.

For reliability testing, one-way analysis of variance (ANOVA) should be performed. In this model, the coefficient of determination (R^2) is used to evaluate the model fit and for assessment of lack of fit in the applied F-test [21]. In this study, the finding of the experiments was entered in the RSM model as design. Moreover, the software Design Expert 11 was used for modeling.

The Monte Carlo method is a computational algorithm that uses random sampling to calculate the results [22]. In the sensitivity analysis of the Monte Carlo simulation method, unlike analytical methods, the work is based on the simulation of the desired phenomenon in large numbers. For this purpose, each of the input parameters was generated in large numbers (in this study 10,000 times) by existing statistical methods and simulated, and by placing them in the created model, the response variable was also generated in the same number. To generate each input parameter, the best statistical distribution was first fitted to each of the input parameters, including contact time, adsorbent dose, ATN concentration, and pH. Table 2 provides the statistical distribution of input parameters and response variable. Then, in the statistics distribution, around 10000 data were generated for input parameters. After that, by the developed RSM model, response variable (ATN removal) was computed for any 10000 set. Finally, sensitivity of response variable to the input parameters was determined based on 10000 existing datasets by the Pearson correlation method [23]. For performance of all of the steps of sensitive analysis, the SPSS 26 software was used.

Table 2: Distribution of input parameters in the model.

Parameter	Unit	Distribution
ATN concentration	mg/L	Weibull ($\alpha = 0.78713$, $\beta = 3.8821$)
Adsorbent dose	mg/L	Uniform (min = 50, max = 200)
Time	min	Uniform (min = 5, max = 90)
pH	—	Uniform (min = 2, max = 11)

2.5. Isotherm of Adsorption. In order to evaluate ATN adsorption by M-MWCNTs, an isotherm study was used through the optimal condition including an initial ATN concentration of 0.5, 1, 2, 5, and 10 mg/L, and the adsorbent dose of 0.15 g/L, a contact time of 60 minutes, and a pH value of 7. The water solubility (S_w) of ATN was approximated as 300 mg/L at pH 7. The isotherm fitting tool software (ISOFIT) was used in accordance with the isotherm parameters with the pilot data. ISOFIT is a software program that matches isotherm parameters to experimental data by the minimization of a weighted sum of squared error (WSSE) objective function [24]. ISOFIT supports several isotherms, containing Brunauer–Emmett–Teller (BET), Freundlich, Freundlich with linear partitioning (F-P), generalized Langmuir–Freundlich (GLF), Langmuir, Langmuir with linear partitioning (L-P), linear Polanyi with linear partitioning, and Toth [25].

2.6. Kinetics of Adsorption. For the analysis of the impact of contact time on the adsorption process, the adsorption kinetics was studied. The adsorption kinetics data were fitted to the pseudo-first-order, pseudo-second-order, and intraparticle diffusion kinetic models as presented in equations (4)–(6) [26]:

Pseudo-first-order:

$$q_t = q_e\left(1 - e^{-K1^t}\right). \quad (4)$$

Pseudo-second-order:

$$q_t = \frac{K_2 q_e^2 t}{\left(1 + K_2 q_e t\right)}. \quad (5)$$

Intraparticle diffusion:

$$q_t = K_p t^{0.5} + I, \quad (6)$$

Where K_1 (1/min), K_2 (g/mg min), and K_p (mg/g$\sqrt{}$min) are the constants rate of the pseudo-first-order, pseudo-second-order, and intraparticle diffusion model, respectively. Meanwhile, q_e and q_t (mg/g) are the adsorption capacities of MWCNTs and M-MWCNTs at equilibrium and time t, respectively.

3. Results and Discussion

3.1. Adsorbent Characteristics. Whereas chemical pretreatment of adsorbents can enhance their surface-active protons and their chemisorption capability [27], we modified MWCNTs by NaOCl solution and ultrasonication. According to the result obtained in our previous study, the

optimum condition was in 30% concentration of NaOCl solution and 15 seconds ultrasonication time. Therefore, modification of MWCNTs was carried out with a 30% NaOCl solution and a contact time of 15 seconds with ultrasonic [7]. Several studies showed that MWCNTs modified by the NaOCl solution is an efficient adsorbent for the removal of some contaminants from the aqueous solution [28–31]. NaOCl solution of 30% with the balanced chlorine concentration increases the adsorbent porosity, which led to improvement in the removal efficiency. Nevertheless, NaOCl concentration of 60%, the increased chlorine oxidizes carbon nanotubes and, therewith, reduce the electrical conductivity [7]. Ultrasonic modification of the adsorbent has numerous advantages such as increased porosity, shortened length of the nanotubes, high performance, short duration, environmental soundness, and increased specific surface area of CNTs [7]. Last, researchers reported appropriate results from applying ultrasonic. Ghasemi et al. investigated adsorption and removal of Pb (II) and Cd (II) from environmental samples by an amino-functionalized silica-coated multiwalled carbon nanotube with using ultrasonic. They obtained satisfactory results (adsorption efficiencies were in the range of 98–104%) [32]. Another study compared acid functionalization of the carbon nanotube via ultrasonic and reflux mechanism, and results revealed functionalization of MWCNTs via ultrasonic bath methods is more desirable and it can result in minimum structural destruction on the surface of MWCNTs [14]. Naghizadeh et al. probed the efficiency of the ultrasonic process in the regeneration of graphene nanoparticles saturated with humic acid. They reported the maximum regeneration efficiency, at a pH of 11 and a regeneration time of 60 min, was 85.37% and 72.47% for frequencies of 60 and 37 kHz, respectively [33].

3.2. RSM Modeling. In this study, by the RSM model, nonlinear quadratic equations were fitted to the test results by multiple regression. For variable selection, parameters with p value <0.1 were kept in the model and other items were deleted. The following equation presents the ATN removal.

$$\begin{aligned} y = {} & 3.963 + 11.834x_1 - 0.199x_2 + 0.530x_3 \\ & - 1.952x_4 - 0.058x_1x_2 - 0.106x_1x_3 \\ & - 0.368x_1x_4 - 6.56 * 10^{-4}x_2x_3 + 0.028x_2x_4 \\ & + 0.044x_3x_4 + 0.103x_1^2 + 1.398 * 10^{-3}x_2^2, \end{aligned} \tag{7}$$

where y, x_1, x_2, x_3, and x_4 stand for the ATN removal, ATN concentration, adsorbent dose, time, and pH, respectively.

The equation in terms of actual factors can be used to make predictions about the response for given levels of each factor. Here, the levels should be specified in the original units for each factor. This equation should not be used to determine the relative impact of each factor because the coefficients are scaled to accommodate the units of each factor and the intercept is not at the center of the design space. Experiment condition and the efficiency of laboratory and predicted removal are given in Table 3.

Figure 1 shows the comparison of the test findings and the predicted results of the proposed model. Figure 1(a) shows the scatter plot of the actual vs. predicted response which is one of the richest forms of data visualization. Here, all the points would be close to a regressed diagonal line and represent the goodness of fit of the model. The normal probability plot of the residuals (Figure 1(b)) is approximately linearly supporting the condition that the error terms are normally distributed and there is not any recognizable outlier.

Analysis of variance (ANOVA) was used to evaluate that the model is significant. Table 4 provides the results of ANOVA analysis of the proposed model for ATN removal under the conditions considered in this study. As given in Table 4, the p value of the model is very low and less than 0.05, which shows that the second-order regression equation was significant for predicting the response variable at the appropriate level [34]. The coefficients R^2, adjusted R^2, predicted R^2, and Adeq precision are given in Table 4. All results indicate the high capability of the model in predicting results.

Another way to evaluate the model is the lack of fit test. If the mathematical model is well fitted to the experimental data, the lack of fit test would be insignificant. Briefly, a model will be well fitted to the experimental data if it presents a significant regression and a nonsignificant lack of fit. In this study, the lack of fit has no significant effect; this means that the model is fitting well to all of the design points. This means that the observed errors are not meaningful and systematic, and it can even be assumed that the selected factors are appropriate for the variable response analysis [35, 36].

Figure 2 shows the three-dimensional (3D) plots of the trend of changes in the initial concentration of atenolol, adsorbent dose, pH, and contact time against removal efficiency according to the output of the RSM model.

3.2.1. Effect of pH. Figure 2(a) shows the adsorption of ATN by M-MWCNTs at various pH. In this experiment pH 2, 4, 7, and 11 were studied. As given in Table 3, at each stage, all of the factors such as the pH value, contact time, ATN concentration, and adsorbent dose are variable. As shown in Figure 2(a), to increase the pH values from 2 to 11, the removal efficiency has gently increased. It was found that the best result was obtained at a pH of 11. The low adsorption at the low pH value could be due to the high concentration and high mobility of H^+ ions, which competed with ATN for the adsorption sites during the sorption process [37]. Ahmadi et al. reported that the optimal pH for Ni (II) ions adsorption on MWCNTs from aqueous solution is 10. They mentioned that it could be attributed to the surface of the MWCNTs and is negatively charged. pH and the Ni (II) ions are positively charged; thus, electrostatic attraction is increased between them which enhanced the removal efficiency [38].

Because removal of ATN at pH from 7 to 11 was negligible, we selected pH 7 as an optimal condition. Under low

Table 3: Test condition and the efficiency of laboratory and predicted removal.

Run	Atenolol concentration (mg/L)	Adsorbent dose (mg/L)	Time (min)	pH	Atenolol concentration at time t (mg/L)	Removal (%)	q_e (mg/g)	Predicted ATN removal (%)
1	5	100	90	2	3.49	30.2	15.1	30.4
2	0.5	150	60	11	0.1	80.0	2.66	79.9
3	10	50	90	11	5.71	42.9	85.7	42.3
4	10	150	20	2	6.63	33.6	22.42	33.8
5	5	150	5	4	3.73	25.2	8.41	25.1
6	0.5	50	5	2	0.48	2.6	0.26	2.8
7	1	200	60	2	0.27	72.6	3.63	50.0
8	1	150	90	7	0.2	79.2	5.28	79.2
9	1	50	20	4	0.85	14.8	2.96	14.4
10	10	100	60	4	6.78	32.2	32.19	32.1
11	0.5	200	90	4	0.1	80.0	2	70.0
12	1	100	5	11	0.88	11.2	1.12	12.9
13	5	200	20	11	2.49	50.1	12.53	50.2
14	10	200	5	7	7.02	29.8	14.87	29.7
15	5	50	60	7	2.79	44.2	44.18	44.4
16	0.5	100	20	7	0.43	12.2	0.61	20.3

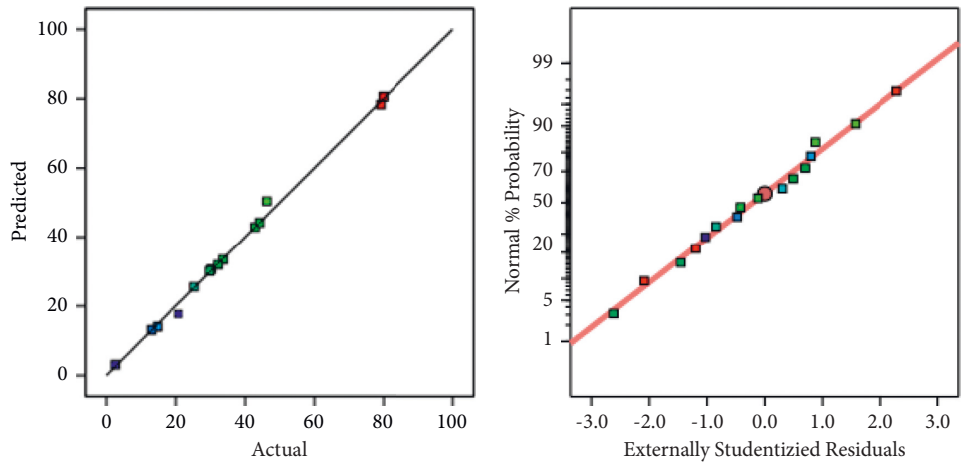

Figure 1: Plot (a) predicted against experimental results and (b) normal probability plot of residuals.

Table 4: ANOVA for the response surface quadratic model.

Source		F value	Pp value	Explanation
ATN removal model				
Model		646.37	<0.0001	Significant
Lack of fit		1.28	0.3402	Not significant
R-squared	0.9996			
Adj R-squared	0.9981			
Predicted R-squared	0.9833			
Adeq precision	81.52			

pH, the H^+ ions can affect or compete against ATN for the adsorption sites. Chang et al. commented that strong and weak adsorption sites, cation exchange, and hydrogen bonding were the adsorption mechanisms for ATN removal by SAz-2 under alkaline conditions [39]. Furthermore, according to our last study on the pH_{ZPC} of the MWCNTs, which was equal to 8, the increase in adsorption of ATN at pH of 7–11 can be linked to pH_{ZPC} [40]. Researchers observed the highest adsorption of benzene, toluene, and p-Xylene at pH 7 too [37]. According to Hu et al., the highest adsorption of ATN on kaolinite occurred in neutral pH [41]. Phenol removal by MWCNTs modified with nitric acid and ultrasonic was studied. Results showed that the highest efficiency of phenol removal was at pH 11 [42]. Hadi et al. revealed that by increasing pH, adsorption of ATN on waste biomass derived activated carbon increased [26].

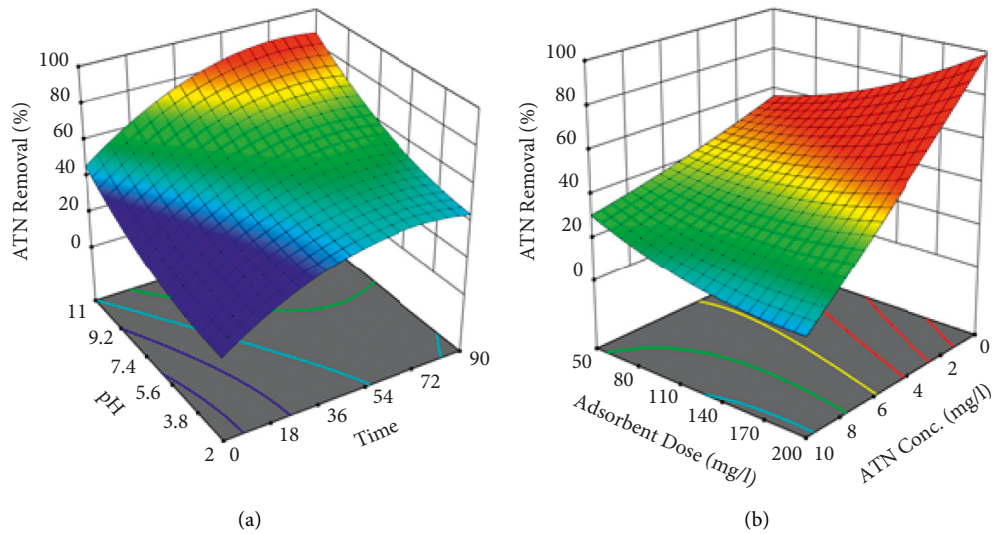

Figure 2: Relation between atenolol removal efficiency and the interaction terms by 3D plot: (a) interaction between pH time; (b) interaction between atenolol concentration-adsorbent dose.

3.2.2. Effect of Contact Time. Figure 2(a) shows the changes in contact time from 5 min to 90 min and increase the ATN removal to about 40%. Increasing trend of the removal efficiency was faster to approximately 60 min, and after that, it was almost constant. This may be due to free adsorption site on nanotubes. In the start of the process, a large amount of sites are free, and as they are occupied by adsorbate, these unoccupied sites tend to decline, resulting to the equilibrium point of the process.

Haro et al.' study confirmed this result for adsorption of ATN on activated carbon [43]. Also, recently, it was reported that with an increase in contact time, removal of benzene, toluene, and p-xylene by multiwalled carbon nanotubes increased [37].

3.2.3. Effect of the Initial Concentration of ATN. As shown in Figure 2(b) the adsorption capacity of ATN on M-MWCNT for initial concentration of ATN from 0.5 mg/L to 1 mg/L slightly increase and after that started to decrease. For the 1 mg/L concentration of ATN, higher removal obtained, and with the enhancement of initial ATN dose, their percentage removal declined. It can be explained at lower concentrations, and ATN molecules have more chance to attach the adsorption sites because the active adsorption sites on the surface of M-MWCNTs is higher than an initial number of ATN molecules, thus removal efficiency increased [44]. With the increase of initial concentration, the limited adsorption active sites were depleted and the adsorption was in a saturated state to reach equilibrium [45]. Because the concentration of 0.5 mg/L was more economical than 1 mg/L, the difference between removal efficiency of them was trifle; therefore, further investigations were conducted by using 0.5 mg/L of ATN.

3.2.4. Effect of Adsorbent Concentration. The adsorbent dosage (50–200 mg/L) as an effective factor in removal efficiency was studied. With the increase of M-MWCNTs dosage from 50 mg/L to 100 mg/L, the adsorption decreased, and after that, when M-MWCNTs dosage raised from 100 mg/L to 200 mg/L, an ascending trend was observed in ATN removal (Figure 2(b)).

This suggests an increase in the number of active sites, the increased contact area, and in turn the enhanced electrostatic interaction which results in the development of removal efficiency [4]. Kończyk et al. observed that with the increased MWCNT dose, due to the surface of adsorbent provided a sufficient number of binding sites for the Pb (II) ions, the adsorption efficiency increased [46]. The maximum adsorption was obtained at 150 mg/L because ATN removal at M-MWCNTs dose between 150 and 200 mg/L was negligible, and it was economical.

Finally, in the current study, optimum condition was 0.5 mg/L ATN initial concentration at 60 min contact time and pH 7 and adsorbent concentration of 150 mg/L.

3.3. Sensitivity Analysis by Monte Carlo Simulation. Sensitivity analysis in a system means how sensitive the predicted variable at the system output is to independent input variables [47]. In this study, sensitivity analysis was performed by the Monte Carlo method. The parameters affecting ATN removal efficiency are time, adsorbent dose, ATN concentration, and pH. Based on 10,000 efficiencies calculated in the Monte Carlo method, the probability distribution diagram for ATN removal is shown in Figure 3. The response parameter followed the gamma probability distribution (scale 0.11, shape 4.73). ATN removal will remove in the range of 5–95% confidence in the range of 14.29–77.80%. Pearson correlation coefficient on 10,000 existing datasets was also used for sensitivity analysis. The test was performed at 95% confidence level in the SPSS software, and its results can be seen in the form of Tornado diagram shown in Figure 4 [48, 49]. According to these graphs, time was the most important parameter, and then, the adsorbent dose and pH had a positive effect on the

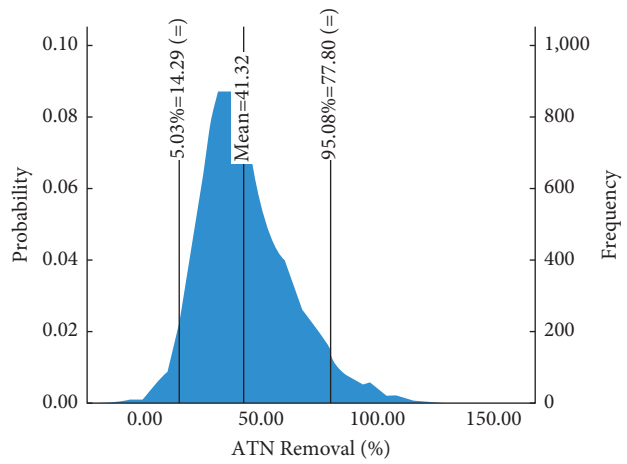

Figure 3: Probability distribution of Monte Carlo simulation output for ATN removal.

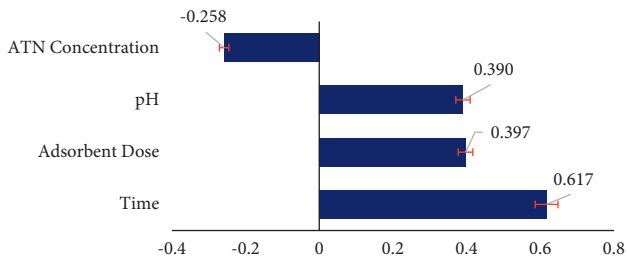

Figure 4: Tornado diagram for sensitivity analysis by the Monte Carlo method.

removal efficiency. Initial concentration and increase of this parameter had a negative effect on pollutant removal efficiency.

3.4. Specifications of the Adsorbent. In our last study, shape, size, and surface morphology of MWCNTs and M-MWCNTs were investigated through the transmission electron microscopy (TEM), and Fourier transform infrared (FTIR) analysis was applied to determine the functional groups and survey the chemical bonds of the modified carbon nanotubes [7]. TEM showed that after modification, ultrasonic reduced the catalytic particles on the surface and increased its specific surface area [50]. FTIR analysis demonstrated various functional groups such as hydroxyl, carboxyl, and carbonyl in raw carbon nanotubes, but in M-MWCNTs, many of the impurities were removed. The most peaks at 1566 and 2352 cm^{-1} in M-MWCNTs are related to the stretching vibration characteristic of C=C and C-O groups, respectively. Also, the peaks at 1708 and 1150 cm^{-1} are associated with the C=O group. According to the study of Pourzamani et al. that experimented modification by ozone and NaOCl, the results showed within the range of 1000–2000, 1500–2500, and 2500–3500 cm^{-1}, the carboxylic, carbonyl, and hydroxyl functional groups have been mainly promoted, respectively [51]. In another study, after modification of MWCNT, it found that peaks at the range of 1563–1652 cm^{-1} were referred to the C=O group [30].

3.5. Adsorption Isotherms. In order to determine the most appropriate isotherm for ATN adsorption by M-MWCNTs, the ISOFIT program was used (Table 5). Isotherm values of correlation between residual and normality (R_N^2), measured and simulated observation (R_y^2), Akaike amended information criterion (AIC_c), and Linssen measure of nonlinearity (M^2) for Freundlich, linear, Polanyi, Langmuir, L-P, and BET are given in Table 5. Based on a fairly low value of AIC_c, atenolol adsorption by M-MWCNTs pursued BET isotherm, and this isotherm is the best fit. The diagram of ATN removal by M-MWCNTs is shown in Figure 5.

It is understood which surface and distribution of sites is uniform and surface is energetically homogeneous, and there is no interaction between adsorbent and adsorbate [52]. Larous and Meniai investigated the adsorption of diclofenac by activated carbon prepared from olive stones, and their results indicate the BET isotherm is fairly better than Langmuir, Freundlich, Temkin, and Dubinin-Radushkevich (D-R) isotherms [53]. Also, this equation was fit for adsorption of a textile dye by nanosized montmorillonite (MMT)/calcium alginate (CA) composite (R^2 value of 0.9855) [54].

Table 6 provides the parameters of BET isotherm related to ATN adsorption on M-MWCNTs, which are results from the ISOFIT software.

In Table 6, the Linssen measure indicates significant WSSE nonlinearity near the optimal parameter values. The statistical measures such as the R_N^2 and Durbin–Watson test (D) show normally distributed weighted residuals with no serial autocorrelation. The ISOFIT provides two standard measures for evaluating isotherm goodness of fit, namely, the root mean squared error (RMSE, equation (8)) and the correlation between measured and fitted observations (Ry, equation (9)).

$$\mathrm{RMSE} = \sqrt{\frac{\mathrm{WSSE}}{(m-p)}}, \tag{8}$$

$$R_y = \frac{\sum_{i=1}^{m}\left(w_i S_{i,\mathrm{obs}} - S_{\mathrm{obs}}^{\mathrm{avg}}\right)\left(w_i S_i - S^{\mathrm{avg}}\right)}{\sqrt{\sum_{i=1}^{m}\left(w_i S_{i,\mathrm{obs}} - S_{\mathrm{obs}}^{\mathrm{avg}}\right)^2 \sum_{i=1}^{m}\left(w_i S_{i,\mathrm{obs}} - S^{\mathrm{avg}}\right)^2}}, \tag{9}$$

where WSSE is the weighted sum of squared error, m is the total number of experimental observations, p is the number of isotherm parameters, w_i is the weight given to observation I; $S_{i,\mathrm{obs}}$ is the i^{th} experimentally measured sorbed concentration; S_i is the i^{th} simulated sorbed concentration computed via an isotherm expression; and $S_{\mathrm{obs}}^{\mathrm{avg}}$ and S^{avg} are the averages of the weighted measured and weighted isotherm simulated adsorbed concentrations, respectively [4].

3.6. Kinetic Studies of the Reaction. A kinetic study was performed to analyse the adsorbed amounts against contact time data by various kinetics models. The pseudo-first-order, pseudo-second-order, and intraparticle diffusion models were used to perform a kinetic study. The plotted kinetic data

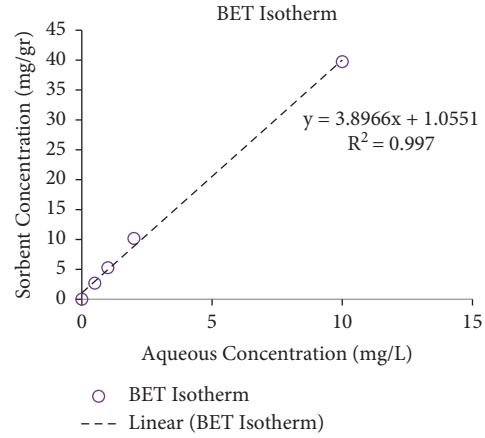

Figure 5: Plot of fitted isotherm (BET) for atenolol adsorption by M-MWCNTS.

Table 5: Summary of selected diagnostics for atenolol adsorbed by M-MWCNT.

Isotherms	AIC_C	R_y^2	R_N^2	M^2	Linearity assessment
Langmuir	3.36	1	0.883	2.09×10^{-4}	Nonlinear
BET	3.27	1	0.881	2.08×10^{-4}	Nonlinear
Linear	6.20	0.998	0.944	1.48×10^{-9}	Linear
L-P	3.36	1	0.880	2.06×10^{-4}	Nonlinear
Freundlich	4.27	1	0.880	9.89×10^{-3}	Nonlinear
Polanyi partition	12.01	0.998	0.990	2.22×10^{-2}	Uncertain

AIC_c, multimodel ranking; R_y^2, correlation between measured and simulated observation; R_N^2, correlation between residual and normality; M^2, Linssen measure of nonlinearity.

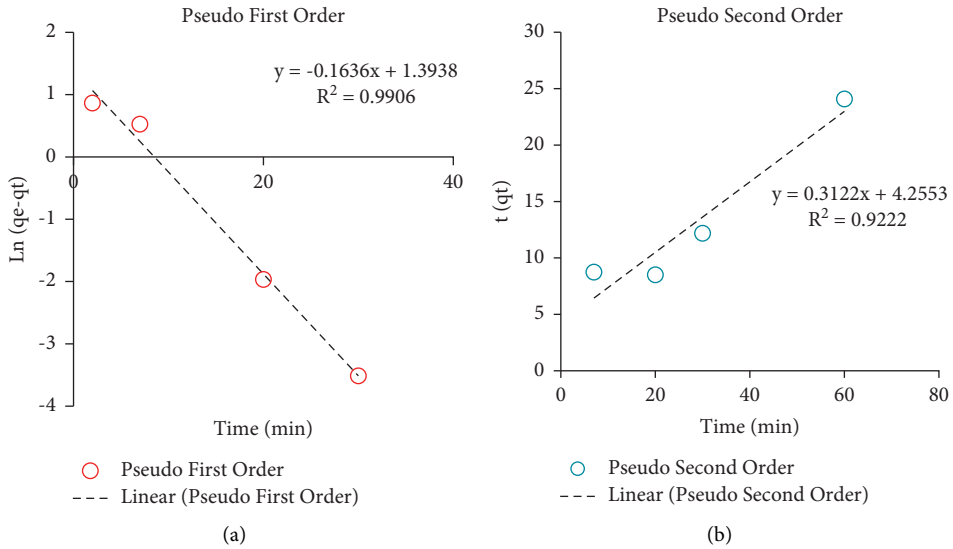

Figure 6: Continued.

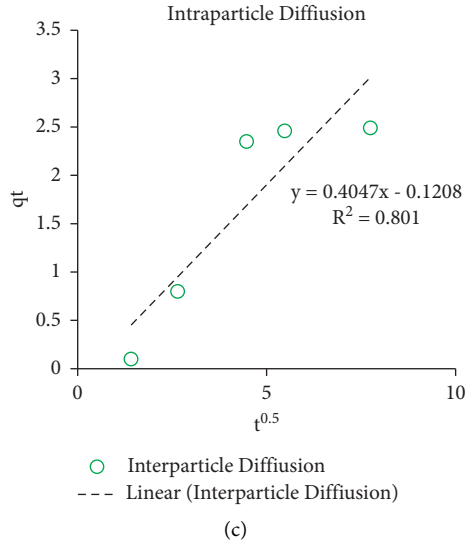

(c)

Figure 6: (a) Plot of pseudo-first-order, (b) pseudo-second-order, and (c) intraparticle diffusion kinetic models for ATN adsorption onto M-MWCNTs.

Table 6: Selected ISOFIT postregression output.

Parameter or statistic		ISOFIT result
Overall quality of fit	WSSE	1.66×10^{-1}
	RMSE	0.235
	R_y	1
Parameter statistics	bQ_0	1.64×10^{3}
	b	1.38×10^{1}
Parameter standard error	bQ_0	5.203×10^{1}
	b	1.409
Test of assumptions Linssen (M^2)	M^2	2.08×10^{-4}
	Threshold	4.73×10^{-3}
	Assessment	Linear
Normality (R_N^2)	R_N^2	0.881
	Critical value	0.71
	Assessment	Normal residuals
Runs test	Number of runs	4
	Pp value	1
	Assessment	No correlation
Durbin–Watson test (D)	D	3.15
	PP value	0.97
	Assessment	No correlation

for ATN on MWCNT-US (Figure 6) illustrate that the pseudo-first-order model better explained the adsorption of atenolol by MWCNT-US because this model has the highest correlation coefficient (R^2 value of 0.9906).

Also, Table 7 provides better agreement of the computed adsorption capacity relevant to the pseudo-first-order kinetic reaction. In this kinetic model, it is assumed that a various rate of adsorbate over time is directly proportional to the saturation concentration and the amount of adsorbent removed over time [55]. In the investigation of the removal of tetracycline antibiotics by a human hair-derived high surface area porous carbon material (HHC), the reaction kinetics also followed first-order kinetics (R^2 values within 0.9859–0.9949) [56]. A similar result was reported by Ali et al. for the uptake of propranolol on ionic liquid iron nanocomposite adsorbent [57]. But in contrast of the results in this study, pseudo-second-order kinetic indicated the best adaptation for the removal of dyes from aqueous solutions by oxygenated functionalities enriched MWCNTs decorated with silica-coated spinel ferrite [58].

Table 8 provides the adsorption capacity of several adsorbents for some pollutants' adsorption. As given in Table 8, MWCNT modified by NaOCl and ultrasonic can be a good alternative adsorbent for the removal of ATN and other pollutants from aqueous solutions.

Table 7: Kinetic parameters for the adsorption of ATN onto MWCNT-US.

Model type	Parameters	Value
Pseudo-first-order model	K_1 (1/min)	0.1636
	q_e (mg/g)	4.03
	R^2	0.9906
Pseudo-second-order model	K_2 (1/min)	0.022
	q_e (mg/g)	3.20
	R^2	0.9222
Intraparticle diffusion	K_p	0.4
	I	0.12
	R^2	0.801

Table 8: Summary of similar studies.

Adsorbent	Adsorbate	Adsorption capacity (mg/g)	Reference
Atenolol	Corncob biochar-based montmorillonite composite	86.86	[1]
Tetracycline	Human hair (carbon material)	128.52	[2]
Ceftriaxone sodium	Nanocomposite g-C_3N_4/MWCNT/Bi_2WO_6 functionalized ultrasound wave	22.357	[3]
Pb(II) ions	MWCNT functionalized by selenophosphoryl groups	156.25	[4]
Atenolol	Ca-montmorillonite	87.89	[5]
Toluene	MWCNT	64.6	[6]
Tetracycline	Purified and oxidized MWCNT	253.3	[7]
Toluene	Single-wall carbon nanotubes-magnetic nanoparticles	6.2–188.9	[8]
Atenolol	M-MWCNTs	2.58	This study

4. Conclusion

Through the removal efficiency analysis of ATN via M-MWCNTs, we found an increase in the adsorbent dose and pH cause increasing of ATN removal efficiency. Time ascending to 60 min promotes the removal efficiency, and after that, it was almost constant. Initial ATN concentration had a negative effect on the removal efficiency. Results showed M-MWCNT is a high-performance adsorbent for removing ATN from the aqueous solution. According to the obtained results from sensitivity analysis, time was the most important parameter, and after that, the adsorbent dose and pH affect positively on ATN removal efficiency.

The kinetic investigation demonstrated that the adsorption process followed the pseudo-first-order model. The result of the isotherm study showed that the process was fitted to the BET model.

Adsorption with M-MWCNT proved to be an efficient method for removing atenolol because this method has high removal efficiency. This method is relatively easy, fast, and eco-friendly. Also, it is possible to reuse MWCNTs, and even their modified mode can be utilized as a new method.

Data Availability

The data generated and analyzed during this study are available from the corresponding author upon request.

Conflicts of Interest

The authors declare that they have no conflicts of interest.

Authors' Contributions

MA conceptualized and conducted the study and revised the article. NB conducted the study and drafted the manuscript. FM conducted the modeling and statistical analysis and revised the manuscript. BD conceptualized and conducted the study and drafted the article. All authors approved the final draft of the manuscript for submission.

References

[1] D. Miao, J. Peng, X. Zhou et al., "Oxidative degradation of atenolol by heat-activated persulfate: kinetics, degradation pathways and distribution of transformation intermediates," *Chemosphere*, vol. 207, pp. 174–182, 2018.

[2] Z. Xu, M. Xie, Y. Ben, J. Shen, F. Qi, and Z. Chen, "Efficiency and mechanism of atenolol decomposition in Co-FeOOH catalytic ozonation," *Journal of Hazardous Materials*, vol. 365, pp. 146–154, 2019.

[3] Y. Wu, Z. Fang, Y. Shi et al., "Activation of peroxymonosulfate by BiOCl@Fe_3O_4 catalyst for the degradation of atenolol: kinetics, parameters, products and mechanism," *Chemosphere*, vol. 216, pp. 248–257, 2019.

[4] B. Dehdashti, M. M. Amin, H. Pourzamani, L. Rafati, and M. Mokhtari, "Removal of atenolol from aqueous solutions by multiwalled carbon nanotubes modified with ozone: kinetic and equilibrium study," *Water Science and Technology*, vol. 2017, no. 3, pp. 636–649, 2018.

[5] Y. Feng, M. Shen, Z. Wang, and G. Liu, "Transformation of atenolol by a laccase-mediator system: efficiencies, effect of water constituents, and transformation pathways," *Ecotoxicology and Environmental Safety*, vol. 183, Article ID 109555, 2019.

[6] J. Hu, X. Jing, L. Zhai, J. Guo, K. Lu, and L. Mao, "BiOCl facilitated photocatalytic degradation of atenolol from water:

reaction kinetics, pathways and products," *Chemosphere*, vol. 220, pp. 77–85, 2019.

[7] B. Dehdashti, M. M. Amin, A. Gholizadeh, M. Miri, and L. Rafati, "Atenolol adsorption onto multi-walled carbon nanotubes modified by NaOCl and ultrasonic treatment; kinetic, isotherm, thermodynamic, and artificial neural network modeling," *Journal of Environmental Health Science and Engineering*, vol. 17, no. 1, pp. 281–293, 2019.

[8] X. Liu, L. Fang, Y. Zhou, T. Zhang, and Y. Shao, "Comparison of UV/PDS and UV/H_2O_2 processes for the degradation of atenolol in water," *Journal of Environmental Sciences*, vol. 25, no. 8, pp. 1519–1528, 2013.

[9] J. Ra, H. Yoom, H. Son, T.-M. Hwang, and Y. Lee, "Transformation of an amine moiety of atenolol during water treatment with chlorine/UV: reaction kinetics, products, and mechanisms," *Environmental Science and Technology*, vol. 53, no. 13, pp. 7653–7662, 2019.

[10] Y.-Q. Gao, N.-Y. Gao, J.-X. Chen, J. Zhang, and D.-Q. Yin, "Oxidation of β-blocker atenolol by a combination of UV light and chlorine: kinetics, degradation pathways and toxicity assessment," *Separation and Purification Technology*, vol. 231, Article ID 115927, 2020.

[11] F. Yu, Y. Li, S. Han, and J. Ma, "Adsorptive removal of antibiotics from aqueous solution using carbon materials," *Chemosphere*, vol. 153, pp. 365–385, 2016.

[12] V. K. Gupta, O. Moradi, I. Tyagi et al., "Study on the removal of heavy metal ions from industry waste by carbon nanotubes: effect of the surface modification: a review," *Critical Reviews in Environmental Science and Technology*, vol. 46, no. 2, pp. 93–118, 2016.

[13] I. Ali, O. M. L. Alharbi, Z. A. ALOthman, A. M. Al-Mohaimeed, and A. Alwarthan, "Modeling of fenuron pesticide adsorption on CNTs for mechanistic insight and removal in water," *Environmental Research*, vol. 170, pp. 389–397, 2019.

[14] L. Y. Jun, N. M. Mubarak, L. S. Yon, C. H. Bing, M. Khalid, and E. C. Abdullah, "Comparative study of acid functionalization of carbon nanotube via ultrasonic and reflux mechanism," *Journal of Environmental Chemical Engineering*, vol. 6, no. 5, pp. 5889–5896, 2018.

[15] X. Hu and Z. Cheng, "Removal of diclofenac from aqueous solution with multi-walled carbon nanotubes modified by nitric acid," *Chinese Journal of Chemical Engineering*, vol. 23, no. 9, pp. 1551–1556, 2015.

[16] M. C. Ncibi and M. Sillanpää, "Optimized removal of antibiotic drugs from aqueous solutions using single, double and multi-walled carbon nanotubes," *Journal of Hazardous Materials*, vol. 298, pp. 102–110, 2015.

[17] E.-R. Kenawy, A. A. Ghfar, S. M. Wabaidur et al., "Cetyltrimethylammonium bromide intercalated and branched polyhydroxystyrene functionalized montmorillonite clay to sequester cationic dyes," *Journal of Environmental Management*, vol. 219, pp. 285–293, 2018.

[18] X. Zhou, Q. Zhang, H. Sun, and Q. Zhao, "Efficient nitrogen removal from synthetic domestic wastewater in a novel step-feed three-stage integrated anoxic/oxic biological aerated filter process through optimizing influent flow distribution ratio," *Journal of Environmental Management*, vol. 231, pp. 1277–1282, 2019.

[19] I. Amalraj Appavoo, J. Hu, Y. Huang, S. F. Y. Li, and S. L. Ong, "Response surface modeling of carbamazepine (CBZ) removal by graphene-P25 nanocomposites/UVA process using central composite design," *Water Research*, vol. 57, no. 57, pp. 270–279, 2014.

[20] R. R. Karri, M. Tanzifi, M. Tavakkoli Yaraki, and J. N. Sahu, "Optimization and modeling of methyl orange adsorption onto polyaniline nano-adsorbent through response surface methodology and differential evolution embedded neural network," *Journal of Environmental Management*, vol. 223, pp. 517–529, 2018.

[21] M. R. Gadekar and M. M. Ahammed, "Modelling dye removal by adsorption onto water treatment residuals using combined response surface methodology-artificial neural network approach," *Journal of Environmental Management*, vol. 231, pp. 241–248, 2019.

[22] T. Salthammer, "Formaldehyde sources, formaldehyde concentrations and air exchange rates in European housings," *Building and Environment*, vol. 150, pp. 219–232, 2019.

[23] H. Lu, E. Kim, and M. Gutierrez, "Monte carlo simulation (MCS)-based uncertainty analysis of rock mass quality *Q* in underground construction," *Tunnelling and Underground Space Technology*, vol. 94, no. 94, Article ID 103089, 2019.

[24] L. S. Matott and A. J. Rabideau, "ISOFIT—a program for fitting sorption isotherms to experimental data," *Environmental Modelling & Software*, vol. 23, no. 5, pp. 670–676, 2008.

[25] H. Pourzamani, M. Hashemi, B. Bina, A. Rashidi, M. M. Amin, and S. Parastar, "Toluene removal from aqueous solutions using single-wall carbon nanotube and magnetic nanoparticle-hybrid adsorbent," *Journal of Environmental Engineering*, vol. 144, no. 2, Article ID 04017104, 2018.

[26] M.-H. To, P. Hadi, C.-W. Hui, C. S. K. Lin, and G. McKay, "Mechanistic study of atenolol, acebutolol and carbamazepine adsorption on waste biomass derived activated carbon," *Journal of Molecular Liquids*, vol. 241, no. 241, pp. 386–398, 2017.

[27] A. Alahabadi, Z. Rezai, A. Rahmani-Sani, A. Rastegar, A. Hosseini-Bandegharaei, and A. Gholizadeh, "Efficacy evaluation of NH4Cl-induced activated carbon in removal of aniline from aqueous solutions and comparing its performance with commercial activated carbon," *Desalination and Water Treatment*, vol. 57, no. 50, p. 23779, 2016.

[28] Y.-C. Chen and C. Lu, "Kinetics, thermodynamics and regeneration of molybdenum adsorption in aqueous solutions with NaOCl-oxidized multiwalled carbon nanotubes," *Journal of Industrial and Engineering Chemistry*, vol. 20, no. 4, pp. 2521–2527, 2014.

[29] H. Pourzamani, I. Parseh, M. Hadei, F. Rashidashmagh, M. Darvish, and S. Fadaei, "Using modified multi-walled carbon nanotubes with ultrasonic homogenizer for BTEX removal from aqueous solutions," *International Journal of Health Studies*, vol. 4, no. 3, 2019.

[30] F. Su, C. Lu, and S. Hu, "Adsorption of benzene, toluene, ethylbenzene and p-xylene by NaOCl-oxidized carbon nanotubes," *Colloids and Surfaces A: Physicochemical and Engineering Aspects*, vol. 353, no. 1, pp. 83–91, 2010.

[31] F. Yu, J. Ma, and Y. Wu, "Adsorption of toluene, ethylbenzene and xylene isomers on multi-walled carbon nanotubes oxidized by different concentration of NaOCl," *Frontiers of Environmental Science & Engineering*, vol. 6, no. 3, pp. 320–329, 2012.

[32] E. Ghasemi, A. Heydari, and M. Sillanpää, "Ultrasonic assisted adsorptive removal of toxic heavy metals from environmental samples using functionalized silica-coated magnetic multiwall carbon nanotubes (magmwcnts@ S_iO_2), engineering in agriculture," *Environment and Food*, vol. 12, pp. 435–442, 2019.

[33] A. Naghizadeh, F. Momeni, and E. Derakhshani, "Efficiency of ultrasonic process in the regeneration of graphene

nanoparticles saturated with humic acid," *Desalination and Water Treatment*, vol. 70, no. 70, pp. 290–293, 2017.

[34] X. Shi, A. Karachi, M. Hosseini et al., "Ultrasound wave assisted removal of ceftriaxone sodium in aqueous media with novel nano composite g-C_3N_4/MWCNT/Bi_2WO_6 based on CCD-RSM model," *Ultrasonics Sonochemistry*, vol. 68, Article ID 104460, 2020.

[35] S. Taherkhani, M. Darvishmotevalli, K. Karimyan, B. Bina, A. Fallahi, and H. Karimi, "Dataset on photodegradation of tetracycline antibiotic with zinc stannate nanoflower in aqueous solution—application of response surface methodology," *Data in Brief*, vol. 19, pp. 1997–2007, 2018.

[36] H. S. Titah, M. I. E. B. Halmi, S. R. S. Abdullah, H. A. Hasan, M. Idris, and N. Anuar, "Statistical optimization of the phytoremediation of arsenic by ludwigia octovalvis- in a pilot reed bed using response surface methodology (RSM) versus an artificial neural network (ANN)," *International Journal of Phytoremediation*, vol. 20, no. 7, pp. 721–729, 2018.

[37] H. Anjum, K. Johari, N. Gnanasundaram, A. Appusamy, and M. Thanabalan, "Investigation of green functionalization of multiwall carbon nanotubes and its application in adsorption of benzene, toluene & p-xylene from aqueous solution," *Journal of Cleaner Production*, vol. 221, pp. 323–338, 2019.

[38] S. Ahmadi, C. A. Igwegbe, S. Rahdar, and Z. Asadi, "The survey of application of the linear and nonlinear kinetic models for the adsorption of nickel(II) by modified multi-walled carbon nanotubes," *Applied Water Science*, vol. 9, no. 4, p. 98, 2019.

[39] P.-H. Chang, W.-T. Jiang, B. Sarkar, W. Wang, and Z. Li, "The triple mechanisms of atenolol adsorption on ca-montmorillonite: implication in pharmaceutical wastewater treatment," *Materials*, vol. 12, no. 18, p. 2858, 2019.

[40] M. M. Amin, B. Dehdashti, L. Rafati, H. R. Pourzamani, M. Mokhtari, and M. Khodadadi, "Removal of atenolol from aqueous solutions by multiwalled carbon nanotubes: isotherm study," *Desalination and Water Treatment*, vol. 133, pp. 212–219, 2018.

[41] Y. Hu, N. M. Fitzgerald, G. Lv, X. Xing, W.-T. Jiang, and Z. Li, "Adsorption of atenolol on kaolinite," *Advances in Materials Science and Engineering*, vol. 2015, Article ID 897870, 8 pages, 2015.

[42] W. Yang, Z. Jiang, X. Hu, X. Li, H. Wang, and R. Xiao, "Enhanced activation of persulfate by nitric acid/annealing modified multi-walled carbon nanotubes via non-radical process," *Chemosphere*, vol. 220, pp. 514–522, 2019.

[43] N. K. Haro, P. Del Vecchio, N. R. Marcilio, and L. A. Féris, "Removal of atenolol by adsorption—study of kinetics and equilibrium," *Journal of Cleaner Production*, vol. 154, no. 154, pp. 214–219, 2017.

[44] S. Mallakpour and S. Rashidimoghadam, "Application of ultrasonic irradiation as a benign method for production of glycerol plasticized-starch/ascorbic acid functionalized MWCNTs nanocomposites: investigation of methylene blue adsorption and electrical properties," *Ultrasonics Sonochemistry*, vol. 40, pp. 419–432, 2018.

[45] C. Fu, H. Zhang, M. Xia, W. Lei, and F. Wang, "The single/co-adsorption characteristics and microscopic adsorption mechanism of biochar-montmorillonite composite adsorbent for pharmaceutical emerging organic contaminant atenolol and lead ions," *Ecotoxicology and Environmental Safety*, vol. 187, Article ID 109763, 2020.

[46] J. Kończyk, S. Żarska, and W. Ciesielski, "Adsorptive removal of Pb(II) ions from aqueous solutions by multi-walled carbon nanotubes functionalised by selenophosphoryl groups: kinetic, mechanism, and thermodynamic studies," *Colloids and Surfaces A: Physicochemical and Engineering Aspects*, vol. 575, pp. 271–282, 2019.

[47] M. Bahrami, M. Akbari, S. A. Bagherzadeh, A. Karimipour, M. Afrand, and M. Goodarzi, "Develop 24 dissimilar ANNs by suitable architectures & training algorithms via sensitivity analysis to better statistical presentation: measure MSEs between targets & ANN for Fe-CuO/Eg-water nanofluid," *Physica A: Statistical Mechanics and Its Applications*, vol. 519, pp. 159–168, 2019.

[48] F. Lionetti, M. Pastore, U. Moscardino, A. Nocentini, K. Pluess, and M. Pluess, "Sensory processing sensitivity and its association with personality traits and affect: a meta-analysis," *Journal of Research in Personality*, vol. 81, pp. 138–152, 2019.

[49] F. Mohammadi, B. Bina, M. M. Amin, H. R. Pourzamani, Z. Yavari, and M. R. Shams, "Evaluation of the effects of alkylphenolic compounds on kinetic parameters in a moving bed biofilm reactor," *Canadian Journal of Chemical Engineering*, vol. 96, no. 8, pp. 1762–1769, 2018.

[50] D. Zhang, L. Shi, J. Fang, X. Li, and K. Dai, "Preparation and modification of carbon nanotubes," *Materials Letters*, vol. 59, no. 29-30, pp. 4044–4047, 2005.

[51] H. Pourzamani, Y. Hajizadeh, and S. Fadaei, "Efficiency enhancement of multi-walled carbon nanotubes by ozone for benzene removal from aqueous solution," *International Journal of Environmental Health Engineering*, vol. 40, no. 1, 2015.

[52] R. Saadi, Z. Saadi, R. Fazaeli, and N. E. Fard, "Monolayer and multilayer adsorption isotherm models for sorption from aqueous media," *Korean Journal of Chemical Engineering*, vol. 32, no. 5, pp. 787–799, 2015.

[53] S. Larous and A.-H. Meniai, "Adsorption of diclofenac from aqueous solution using activated carbon prepared from olive stones," *International Journal of Hydrogen Energy*, vol. 41, no. 24, p. 10380, 2016.

[54] A. Hassani, R. D. C. Soltani, S. Karaca, and A. Khataee, "Preparation of montmorillonite-alginate nanobiocomposite for adsorption of a textile dye in aqueous phase: isotherm, kinetic and experimental design approaches," *Journal of Industrial and Engineering Chemistry*, vol. 21, pp. 1197–1207, 2015.

[55] M. T. Samadi, R. Shokoohi, M. Araghchian, and M. Tarlani Azar, "Amoxicillin removal from aquatic solutions using multi-walled carbon nanotubes," *Journal of Mazandaran University of Medical Sciences*, vol. 24, no. 117, pp. 103–115, 2014.

[56] M. J. Ahmed, M. A. Islam, M. Asif, and B. H. Hameed, "Human hair-derived high surface area porous carbon material for the adsorption isotherm and kinetics of tetracycline antibiotics," *Bioresource Technology*, vol. 243, pp. 778–784, 2017.

[57] I. Ali, Z. A. Alothman, and A. Alwarthan, "Uptake of propranolol on ionic liquid iron nanocomposite adsorbent: kinetic, thermodynamics and mechanism of adsorption," *Journal of Molecular Liquids*, vol. 236, pp. 205–213, 2017.

[58] S. M. Wabaidur, M. A. Khan, M. R. Siddiqui et al., "Oxygenated functionalities enriched MWCNTs decorated with silica coated spinel ferrite—a nanocomposite for potentially rapid and efficient de-colorization of aquatic environment," *Journal of Molecular Liquids*, vol. 317, Article ID 113916, 2020.